An New Area Function for Sharp Indenter Tips in Nanoindentation

LIU Dong-xu, ZHANG Tai-hua

(LNM, Institute of Mechanics, Chinese Academy of Sciences, Beijing 100080, China)

Abstract: A new area function is introduced and applied to a Berkovich tip in order to characterize the contact projected area between an indenter and indented material. The function can be related directly to tip-rounding, thereby having obviously physical meaning. Nanoindentation experiments are performed on a commercial Nano Indenter XP system. The other two area functions introduced by Oliver and Pharr and by Thurn and Cook respectively are involved in this paper for comparison. By comparison from experimental results among different area functions, the indenter tip described by the proposed area function here is very close to the experimental indenter.

Key words: indentation; indenter; contact area; area function; tip-rounding

一种标定纳米硬度计压针面积函数的新方法. 刘东旭, 张泰华. 中国航空学报(英文版), 2004, 17(3): 159 - 164.

摘　要:为了研究纳米硬度计压针尖端曲率半径对面积函数的影响,提出一个基于几何方法建立的压针面积函数。这个函数在接触面积和压针曲率半径之间建立了直接的联系,具有明显的物理意义。通过纳米硬度计 Nano Indenter XP 的压痕试验来检查此面积函数的有效性,并将这个面积函数的测试结果与其他两种已有的用不同方法确定面积函数测试结果对比,说明这里提出的这个压头面积函数能很好地描述试验中的实际压头。

关键词:压痕;接触面积;面积函数;尖端曲率;硬度

文章编号: 1000-9361(2004)03-0159-06　　**中图分类号**: V250.3; TH140.2　　**文献标识码**:A

In the past two decades, nanoindentation, also known as depth-sensing indentation (DSI), continuous-recording indentation and ultra-low-load indentation, has been developed as an important technological tool for measuring the mechanical properties of bulk materials, thin films and coatings, especially at small scales. The technique, called depth-sensing method, relies on high-resolution instrument that continuously monitor the loads and displacements of an indenter as it is pushed into and withdrawn from a material. Many mechanical properties, most commonly, the hardness and elastic modulus, can be derived through analyzing the load-displacement curve obtained during loading and unloading[1], which is schematically illustrated in Fig. 1. Conventional micro-hardness by imaging of a residual indentation impression to estimate the contact area at peak load is determined. But, for small-scale indentation, measuring the residual impression may be extremely difficult, not only requiring the use of sophisticated imaging techniques such as scanning electron microscopy, scanning probe microscopy, or transmission electron microscopy, but being too blurry to measure the contact area exactly for indentation edges of some materials[2]. However, if the projected contact area is a known function of the indentation depth, *i. e*,

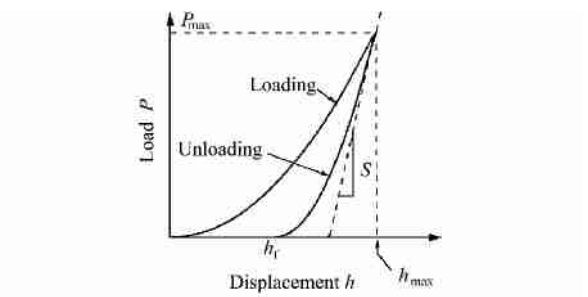

Fig. 1　A typical load-displacement curve

Received date: 2003-08-14; Revision received date: 2004-03-12
Foundation items: National Natural Science Foundation of China (10372103, 10172086); Chinese Academy of Sciences (KJCX2-SW-L2)

area function, no imaging is required, and the contact depth at peak load can be extracted from indentation load-displacement curves (Fig. 1). Knowing the projected contact area, the hardness H and the reduced modulus E_r are derived from

$$H = \frac{P_{max}}{A_c} \quad (1)$$

and

$$E_r = \frac{\sqrt{\pi}}{2\beta}\frac{S}{\sqrt{A_c}} \quad (2)$$

where P_{max} is the peak load, A_c is the projected contact area, S is the unloading stiffness measured at the maximum depth of penetration h_{max}, β is a constant that depends on the indenter geometry. The reduced modulus is employed in order to account for the fact that elastic deformations occur in both the indenter and the specimen. E_r may also be given by

$$E_r = \left(\frac{1-\nu^2}{E} + \frac{1-\nu_i^2}{E_i}\right)^{-1} \quad (3)$$

where E, E_i and ν, ν_i are Young's modulus and Poisson's ratio of the specimen and indenter, respectively[3]. As it is well known, all indenters in practice have a certain degree of tip-rounding. This deviation of an experimental indenter from perfect sharp is the most significant source of uncertainty in nanoindentation testing results[4]. Indeed, determining the contact area from the indentation load and displacement is central to study the properties of materials by nanoindentation[5].

In this paper a new area function for sharp indenter tips considered as geometry of concrete shape is propounded. Nanoindentation experiments conducted on several specimens are used to check the performance of the area function. The experimental results of the current area function would be compared with those determined from two area functions proposed by others.

1 Approaches of Determining Area Function

Several approaches have been developed to calibrate the indenter tip area-depth function. These include three kinds: imaging techniques[5,6], iteration techniques[1,4] and geometry techniques[7].

Except for directly measuring the residual indentation impression, alternative technique is the direct measurement of the indenter using a scanning force microscopy (SFM), calculating the contact area from scan points[4]. Because of requiring sophisticated imaging tools at small scales and limitation of laboratory conditions, even at the deep indentation depth, imaging techniques are time consuming. In addition, the contact area by imaging techniques may vary with different people who measure the dimensions of indentation impressions.

And on the iteration technique, the method proposed by Oliver and Pharr is a typical example[1] making iteration procedure between area function and frame compliance, which involves the use of several standard specimens and the evaluation of unloading stiffness, and finally an eight-parameter area function is proposed as expressed by

$$A_c = \frac{\pi}{\cot^2\alpha}h_c^2 + \sum_{i=1}^{8} C_i h_c^{1/2^{i-1}} \quad (4)$$

where h_c is the contact depth at the peak load, α is the effective included half-angle, C_1-C_8 which are used to describe the tip-rounding are constants. Although the analysis technique developed by Oliver and Pharr is very widely used for analyzing nanoindentation load displacement data, there are several problems as follows. Firstly, the iterative process may be difficult to achieve convergence without accurately knowing the frame compliance, and the initial guess for the iteration often affects the determination of the area function. Secondly, to maintain the reproducibility of the experimental results, it is necessary to periodically calibrate the area function because of indenter tip-wearing with increase of experimental times. Thirdly, the area function varies with materials even if the same indenter is used[8]. A combined iteration technique[4] based on Oliver and Pharr method is proposed by Herrmann and Jennett *et al*, however, it requires considerable experimental effort.

Geometry techniques directly depend on the geometry relations of indenter tip. Thurn and Cook take the profile of the indenter tip as the harmonic average of these two limits: a conical tip and a

spherical tip[6,9]. The conical tip can be described by

$$z_1 = r\cot a \quad (5)$$

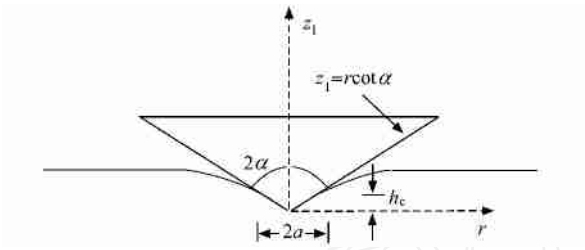

(a) cone of included angle 2α

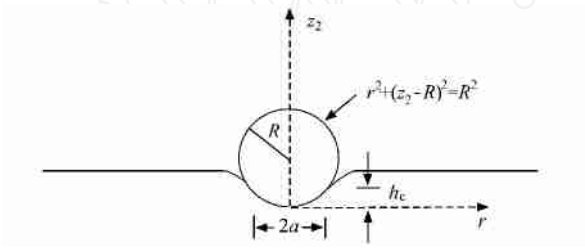

(b) sphere of radius R

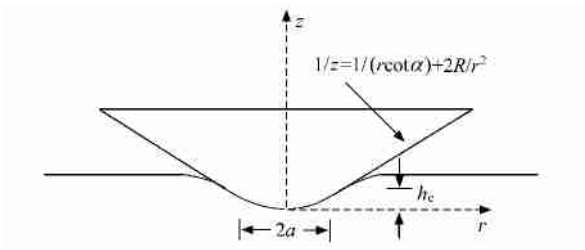

(c) the harmonic average (a) and (b)

Fig. 2 Schematic diagrams of solids of revolution describe indenter tips:

as shown in Fig. 2(a). Fig. 2(b) shows a spherical indenter with a sphere radius R. Generally, if $r \ll R$,

$$z_2 \approx \frac{r^2}{2R} \quad (6)$$

from geometry, then the harmonic average of a spherical tip described by Eq. (6) at small penetration depths and a conical tip described by Eq. (5) at large penetration depths is expressed by

$$\frac{1}{h_c} = \frac{1}{z_1(a)} + \frac{1}{z_2(a)} = \frac{1}{a\cot\alpha} + \frac{2R}{a^2} \quad (7)$$

where a is the contact radius. Eq. (7) can be re-written as

$$h_c = a\cot\alpha\left(1 + \frac{2R\cot\alpha}{a}\right)^{-1} \approx a\cot\alpha - 2R\cot^2\alpha \quad (8)$$

The contact area function of the indenter tip can be determined from Eq. (8) at a given contact depth,

$$A_c = \pi a^2 = \pi\left(\frac{h_c}{\cot\alpha} + 2R\cot\alpha\right)^2 \quad (9)$$

The condition $(a/(2R)) > \cot\alpha$ must be met so that the contact $h_c > 0$ in Eq. (8) is satisfied. Not only has the area function physical meaning to a certain extent, but also can be related directly to tip-rounding. However, accurately measuring the radius R whose value varies with tip-wearing may require some efforts. Experimental results of this area function will be discussed in Part 3.

2 Introducing a New Area Function

Sharp indenters are commonly used in nanoindentation, and it is often convenient to model their behavior by that of the cone wtih a included half-angle which gives the same area-to-depth relationship. For the Berkovich and Vickers pyramids, the equivalent cone half-angle is 70.3° because of the geometric self-similarity of pyramidal indenters[10]. Any area function for indenters is intended to calibrate the tip-rounding. Although Eq. (4) has a good performance verified by experiments, there are too many parameters involved without definitely physical meaning and required to be determined. Eq. (9) is gotten based on the geometry of indenter, which is not quite intuitional. In this paper, the indenter is taken as a more concrete geometry shown in Fig. 3 which can directly describe the profile of the indenter, and now this geometry has been admitted by some researchers[11-13]. Then, the area function for an indenter tip can be determined from the geometric relation existing in this geometry (Fig. 3).

The contact radius a is the sum of a_1 and a_2 (Fig. 3). According to the relations of this geometry (Fig. 3),

$$a_1 = R\cot\alpha \quad (10)$$

$$a_2 = \tan\alpha[h_c - R(1 - \sin\alpha)] \quad (11)$$

Then,

$$a = a_1 + a_2 = \tan\alpha[h_c - R(1 - \sin\alpha)] + R\cos\alpha \quad (12)$$

Thus, an area function for indenter tips is gotten from Eq. (12),

$$A_c = \pi a^2 = \pi\left[\frac{h_c}{\cot\alpha} + R\left(\frac{1-\sin\alpha}{\cos\alpha}\right)\right]^2$$

i. e,

$$A_c = \frac{\pi h_c^2}{\cot^2\alpha} + \frac{2\pi RBh_c}{\cot\alpha} + \pi R^2 B^2 \quad (13a)$$

where

$$B = \frac{1-\sin\alpha}{\cos\alpha}$$

The first term of the right side of Eq. (13a) describes a perfect pyramidal indenter, and the second is perturbation describing tip-rounding. As for the third term, it prevents the projected contact area from going to zero as the contact depth approaches zero, which becomes significant with respect to A_c only at extremely shallow indentation where the tip is primarily sphere-like. The condition

$$h_c > R(1-\sin\alpha) \quad (14)$$

is necessary to assure $a_2 > 0$. For sharp indenter, it is impossible that the contact indentation depth[1],

$$h_c = h_{max} - \varepsilon\frac{P_{max}}{S} \quad (15)$$

where ε is a constant related to indenter geometry, will approach zero from indentation curves under the condition that Eq. (14) is satisfied. The ratio of the actual contact area to the perfect indenter contact area will increase with the depth decrease[14]. So, what is important to the third term of Eq. (13a) is to predict the comparatively accurate contact area at small depth.

The difference between Eq. (13a) and Eq. (9) can be easily found to be that $2\cot\alpha$ is greater than B. The first reason is that the condition of $a \ll R$ might be not met with the depth increase. The second is that the two kinds of geometry models are variant, of which one is assumed with the cone surface to be tangent to the sphere surface (Fig. 3), and the another is not. As a result, the contact area of Eq. (9) is always larger than that of Eq. (13a), which becomes more evident at very shallow depth.

For the purpose of fitting curve, this area function can also be expressed as

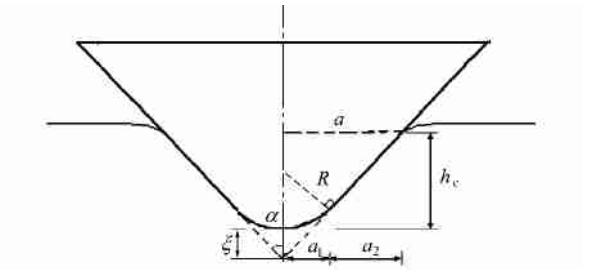

Fig. 3 Schematic diagram showing the geometry of an identer with tip-rounding

$$A_c = \left(\frac{h_c}{m} + n\right)^2 \quad (13b)$$

where m is a fitted parameter related to α, and n is a parameter related to α and R. This equation is very similar to the following one introduced by Herrmann and Jennett *et al*,

$$\sqrt{A_c} = ch_c + b, \quad (16)$$

with c and b as regression coefficients[4].

3 Experimental Results

In order to check the validity of the current proposed area function (Eq. (13a)) for the sharp indenter, nanoindentation experiments are performed by using a commercial Nano Indenter XP system which has a displacement resolution of 0.01 nm and a load resolution of 50 nN. A Berkovich indenter is used to carry out all the indentation tests. Three materials are indented: fused silica, aluminum and copper.

At least five indentations are performed at each load. Fig. 4 and Fig. 5 shows the hardness H and the elastic modulus E respectively, which are determined from three different area functions presented above. In these legends, 'O & P' denotes the results calculated from the area function proposed by Oliver and Pharr, 'T & C' from the area function proposed by Thurn and Cook, and 'L & Z' from proposed area function in the paper.

From these results, it can be found that the agreement of hardness and modulus obtained from the three area functions is excellent at the deep indentation depth. At lower depths, the results obtained from the current proposed area function are nearly consistent with those from the area function of Oliver and Pharr, which can be explained by the

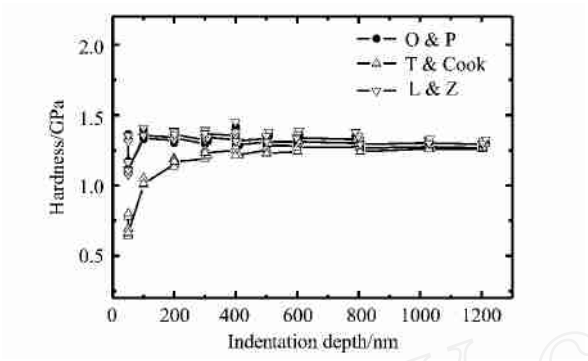

(a) Aluminum

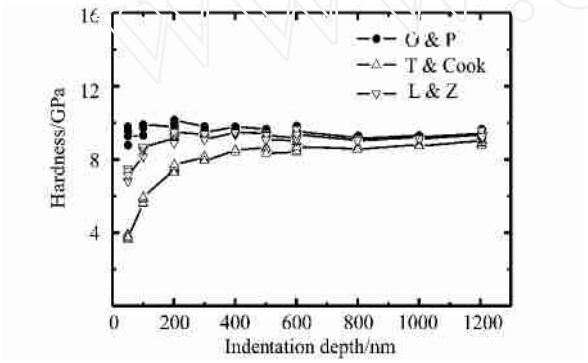

(b) Fused silica

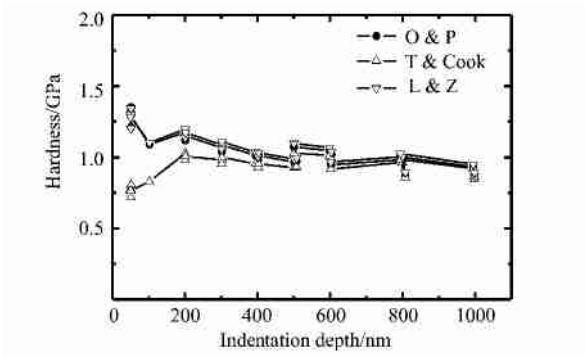

(c) Copper

Fig. 4 Hardness of materials determined from diferent area functions

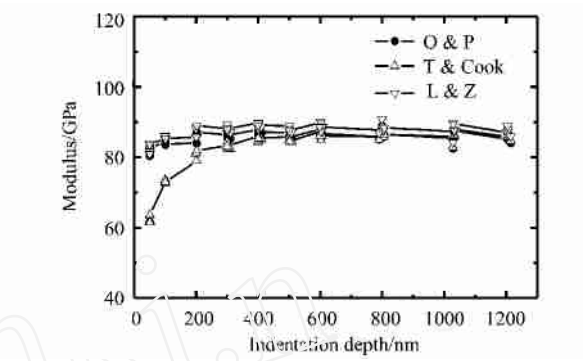

(a) Aluminum

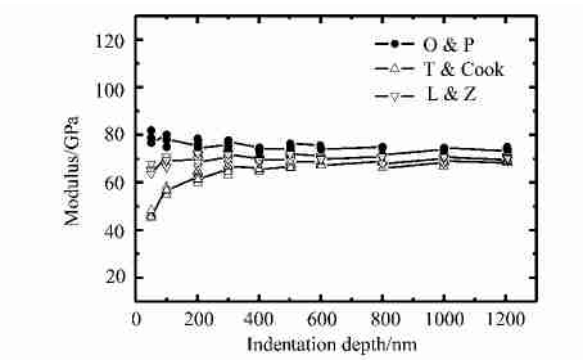

(b) Fused silica

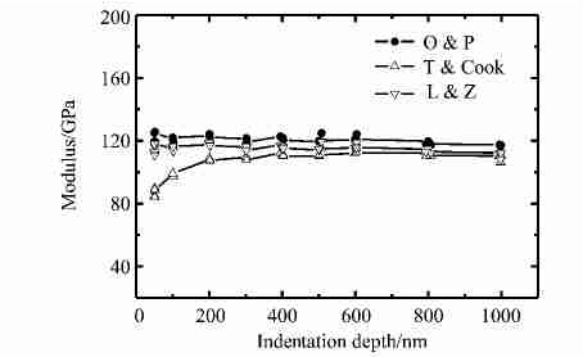

(c) Copper

Fig. 5 Modulus of materials determinde from different area functions

condition (14) because h_c only need to be greater than 17 nm even if $R = 100$ nm. However, the results of fused silica from current area function deviated from that from Oliver & Pharr's area function at 50 - 100 nm. This will not compromise the validity of current area function because, as is so often pointed out, the measurements of load and displacement are susceptible to many interfering factors[14] other than tip-rounding of indenter at small scales. Both hardness and modulus exhibit the tendency in which the contact area determined from Eq. (9) proposed by Thurn and Cook increases with the decrease of the indentation depth, even meeting the condition of $a/(2R) > \cot\alpha$. This proves the analysis in Part 2.

4 Conclusions

Thinking of the profile of a sharp indenter as a concrete geometry, a physically meaningful area function is obtained. And the function is compared with the area function proposed by Oliver and Pharr which has been adopted as a standard reference method in ISO-14577. The function is easy to be determined as compared with eight-parameter

area function. On examination of the analysis of indentation experiments, it is seen that the current proposed area function describes the indenter tip very well, especially at lower indentation depths.

Certainly, the function has the same problem in determining the radius R. As to the determination of the radius, please refer Ref. [9] and Ref. [11]. However, once the radius is known, it will be admitted here and will not change in one experiment or even in those of a period.

References

[1] Oliver W C, Pharr G M. An improved technique for determining hardness and elastic modulus using load and displacement sensing indentation experiments [J]. J Mater Res, 1992, 7(6): 1564 - 1583.

[2] Zhang T H, Liu D X, *et al*. Micro/ Nanomechanical and tribological properties of thin diamond-like carbon coatings[J]. Chinese Journal of Aeronautics, 2003, 16(1): 47 - 51.

[3] **张泰华, 杨业敏. 纳米硬度技术的发展和应用**[J]. **力学进展**, 2002, 32(3): 349 - 364.
Zhang T H, Yang Y M. Developments and application of nano-hardness techniques[J]. Advances in Mechanics, 2002, 32(3): 349 - 364. (in Chinese)

[4] Herrmann K, Jennett N M, *et al*. Progress in determination of the area function of indenters used for nanoindentation[J]. Thin Solid Films, 2000, 377 - 378: 394 - 400.

[5] McElhaney K W, Vlassak J J, Nix W D. Determination of indenter tip geometry and indentation contact area for depth-sensing indentation experiments[J]. J Mater Res, 1998, 13(5): 1300 - 1306.

[6] Pethica J B, Hutchings R, Pethica J B, *et al*. Hardness measurement at penetration depths as small as 20 nm[J]. Phil Mag A, 1983, 48(4): 593 - 606.

[7] Thurn J, Cook R F. Simplified area function for sharp indenter tips in depth-sensing indentation[J]. J Mater Res, 2002, 17(5): 1143 - 1146.

[8] Sawa T, Tanaka K. Simplified method for analyzing nanoindentation data and evaluating performance of nanoindentation instruments[J]. J Mater Res, 2001, 16(11): 3084 - 3096.

[9] Thurn J, Morris D J, Cook R F. Depth-sensing indentation at macroscopic dimensions[J]. J Mater Res, 2002, 17(10): 2679 - 2690.

[10] Pharr G M, Bolshakov A. Understanding nanoindentation unloading curves[J]. J Mater Res, 2002, 17(10): 2660 - 2671.

[11] Sun Y, Zheng S, *et al*. Indenter tip radius and load frame compliance calibration using nanoindentation loading curves [J]. Phil Mag Lett, 1999, 79(9): 649 - 658.

[12] Cheng Y T, Cheng C M. Further analysis of indentation loading curves: effects of tip rounding on mechanical property measurements[J]. J Mater Res, 1998, 13(4): 1065 - 1067.

[13] **李敏, 梁乃刚, 张泰华, 等. 纳米压痕过程的三维有限元数值试验研究**[J]. **力学学报**, 2003, 35(3): 257 - 264.
Li M, Liang N G, Zhang T H, *et al*. 3D finite element simulation of the nanoindentation process[J]. Acta Mechanica Sinica, 2003, 35(3): 257 - 264. (in Chinese)

[14] Fisher-Cripps A C. Nanoindentation [M]. New York: Spring-Verlag, 2002.

Biographies:

LIU Dong-xu Born in 1979, now a graduate student in the State Key Lab of Nonlinear Mechanics, Institute of Mechanics, Chinese Academy of Sciences.
E-mail: liudx@lnm.imech.ac.cn

ZHANG Tai-hua Born in 1966, he received B. S. from University of Science and Technology of China in 1990 and M. S. form Xi'an Jiaotong University in 1995, respectively. He received Ph. D. from Institute of Mechanics in 1999. He has published more than 30 scientific papers in various periodicals.
Tel: (010) 62541733
E-mail: zhangth@lnm.imech.ac.cn